Energy spectrum and flux of fast neutrons in the atomsphere

R. N. St. Onge*
Physics Department, University of New Hampshire, Durham, New Hampshire 03824
(Received 12 March 1974; revised manuscript received 3 January 1977)

The energy spectrum of fast neutrons (5–20 MeV) in the atmosphere at the Pfotzer maximum (~ 100 g/cm^2) was measured at geomagnetic latitude 42°N ($P_c = 4.4$ GeV). The n-γ detector was a 4.6×4.65-cm cylindrical cell of organic liquid scintillator (NE213) coupled to a high-resolution, two-parameter, multiparticle pulse-shape discriminator with a two-parameter (64×64) logarithmic pulse-height analyzer. An anticoincidence charged-particle shield completely enclosed the n-γ detector. The spectral parameter $\beta(E)$ of the differential neutron energy spectrum decreased from 4.4 ± 0.8 in the range 3.5–6.0 MeV to 1.5 ± 1.0 in the range 11–20 MeV. The integrated neutron flux at Pfotzer maximum between 3.5 and 10.0 MeV was 0.36 ± 0.10 neutrons/cm^2 sec. The implications of these results for the high-energy albedo neutron leakage as a source of the energetic proton flux in the radiation belts are discussed.

I. INTRODUCTION

Neutrons in the earth's atmosphere are produced by the interaction of both galactic and solar cosmic rays with air nuclei. An investigation of the energy spectrum and flux of the neutrons from both of these sources is important for several reasons: (1) An energetic neutron escaping from the atmosphere can decay into a proton and an electron within the magnetosphere and then these may be trapped by the geomagnetic field to contribute to the radiation belts[1]. (2) The capture of neutrons by atmospheric nitrogen is responsible for the production of the age-dating nucleus ^{14}C through the reaction ^{14}N$(n, p)^{14}$C. (3) The fast neutrons are related to the energy spectrum of the galactic cosmic rays. A comprehensive review of atmospheric neutrons has been given by Schopper *et al.*[2] and Lockwood.[3]

Any evaluation of the contribution made by the neutron leakage to the population of energetic protons in the inner radiation belt depends upon a knowledge of the neutron energy spectrum and flux at the top of, or above, the atmosphere. Calculations have been made of the intensity and energy spectrum of the neutron leakage.[4-6] Dragt *et al.*[7] and Hess and Killeen[8] have used these calculations to determine quantitatively the contributions to the radiation belts. These calculated results agree that this source mechanism is inadequate for trapped protons with $E < 20$ MeV. However, the recent neutron measurements of White,[9] Lockwood *et al*;[10] and Kanbach *et al.*[11] in the every range 20 to 400 MeV indicate that the neutron source mechanism is sufficient to provide the observed trapped protons in the range from 20 to 400 MeV.

Direct experimental evidence on the neutron energy spectrum near the top of the atmosphere is essentially limited to measurements of Haymes,[12] Holt *et al.*,[13] Mendell and Korff,[14] Albernhe and Talon,[15] Jenkins *et al.*,[16] Klumper *et al.*,[17] and Preszler *et al.*[18] Most of these measurements were made with recoil-proton detectors using a combinabion of two scintillators which have different pulse rise times and pulse-shape discrimination (PSD) on the inner detector to separate neutrons from γ rays and charged particles.

The present experiment was designed to measure the neutron energy spectrum and flux in the energy interval 3.5–20 MeV. The neutron detector utilized a separate charged-particle rejection scheme and a two-parameter display system for the PSD which separates γ rays from neutrons. In this article the neutron energy spectrum and flux measured during a balloon flight on 7 September 1968 from Palestine, Texas, are presented with some discussion of the novel experimental techniques used.

II. EXPERIMENTAL SYSTEM

A major difficulty encountered in determining the secondary neutron decay population in the atmosphere is to reliably detect a small flux of fast neutrons in a much larger background flux of γ rays and charged particles. To accomplish this, the counter logic first separated the particles into two groups: charged and neutral. Second, the neutral particles were separated into their predominant components: γ rays and neutrons. Experimentally the charged particles were separated from the neutral particles by placing the neutron and γ-ray detector inside a thin, hollow, 4π enclosure of plastic scintillator. The neutral-particle detector, contained within this closed shell, was gated off whenever a charged particle passed through the shield. The n-γ detector separated the γ rays and neutrons by means of their different light-pulse shapes in an organic liquid scintillating cell.

A. The charged-particle identifying system

The hollow, 4π, charged-particle anticoincidence shield of plastic scintillator (NE102) is shown in Fig. 1. It was monitored by two photomultipliers with hemispherical photocathodes (RCA C70132A). The wall thickness of the shield was greater at larger distances from the phototubes to allow particles which enter the shield farther from the photomultipliers to generate a larger scintillation. This compensates for the greater light attenuation in the scintillator for these events.[19] For the most effective use of such a 4π shield the parallel sum and coincidence logic scheme shown in Fig. 2 was included.

This unusual precaution allowed the detection in the case where a high-energy proton interacts inside the shield through charged exchange and a neutron emerges. The worst case is for an event occurring equidistant from the two photomultipliers and generating small, approximately equal, signals in the two photomultipliers and the coincidence gate would be triggered. For charged particles interacting at other places in the shield, the charged-particle flux would be monitored by the summing or coincidence circuits or both.[19]

In order to ascertain quantitatively the rejection efficiency of the shield for charged particles, the preflight test with cosmic-ray secondary muons was conducted. The measured effectiveness was greater than 99.9%. The limitation on the measured effectiveness was due to spurious events occurring during the long time intervals required when using the secondary cosmic-ray muon beam.

B. The neutral-particle-component n-γ identifying system

The n-γ separation was made by the pulse-shaped discrimination of an organic liquid scintillator (NE213) viewed by a fast photomultiplier (RCA 8575). The PSD system[20] compared the integrated scintillation light yield ($\int L\,dt$) with the slow-decay component of the scintillation (dL/dt) in the cylindrical liquid scintillator of (4.6×4.65)-cm diameter. The photomultiplier (PM) pulses were fed to a high-resolution, multiparticle pulse-shape discriminator (PSD) and were subsequently analyzed and digitized by a logarithmic, two-parameter (64 $\times$ 64) pulse-height analyzer (PHA). The effectiveness of the PSD for separating γ rays and neutrons can be seen quantitatively in Figs. 3 and 4. In Fig. 3 the two-parameter PSD data from an AmBe neutron γ-ray source are plotted for a laboratory prototype. The scale in Fig. 3 for both dL/dt and $\int L\,dt$ channels is *different* from that used in the actual flight. Figure 4 is obtained by taking a section of Fig. 3 at the $\int L\,dt$ value for the ^{60}Co Compton edge from 1.17-MeV γ rays. It should be stressed

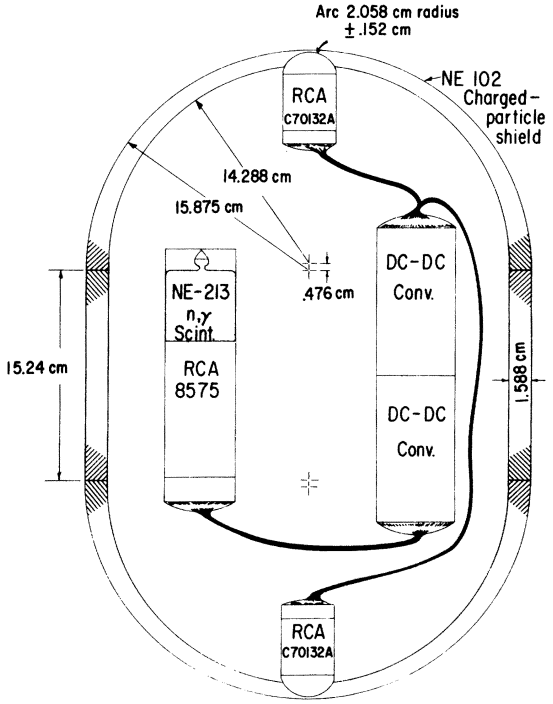

FIG. 1. Charged-particle anticoincidence shield design.

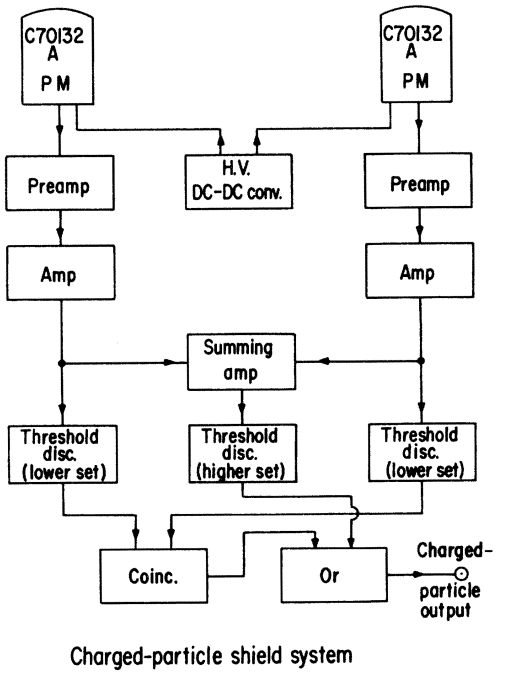

FIG. 2. Parallel sum and coincidence logic of the charged-particle shield system.

that the effectiveness of the PSD circuit to separate neutrons from γ rays over a wide energy range is one of the most important factors in determining accurately the neutron energy spectrum in the atmosphere.

An in-flight calibrator (IFC) was incorporated into the neutron detector by optically coupling to the NE213 scintillator a small (~3 × 3-mm diameter) crystal of NaI(Tl) doped with a radioactive salt of the α emitter ^{241}Am. The much slower NaI(Tl) scintillations resulting from these doped α particles were readily pulse-shape-discriminated from the neutron and γ-ray events shown in Fig. 3.

III. MEASUREMENTS

The raw data from the balloon flight, recorded from 4.7 km (541 mbar) to 19.2 km (62 mbar), are shown in Fig. 5 as a two-parameter ($\int L\,dt \times dL/dt$) pulse-height spectrum. It can be seen that the PSD system separated four different scintillation pulse shapes. These correspond to Compton electrons, recoil protons, α particles from (n, α) reactions and from the IFC. The first three groups of secondary particles result from neutral particles, either neutrons or γ rays, interacting in the organic scintillator with hydrogen or carbon nuclei. The Compton electrons arise from γ-ray interactions with atomic electrons, and the recoil protons are produced by H(n, p)n^1 and ^{12}C(n, p)^{12}B reactions. The α particles are produced by ^{12}C(n, α)^{9}Be and ^{12}C(n, 3α)n^1 reactions. Each of these secondary charged particles was considered in deriving the neutron energy spectrum. The group marked IFC in Fig. 5 corresponds to ^{241}Am α-particle interactions in NaI.

The individual groups of particles (e, p, α, IFC) separated in Fig. 5 were extracted to obtain pulse-height spectra. However, since the data shown are the average over a large range of altitudes (541–62 mbar), the pulse-height spectra were examined for changes in spectral shape with altitude. None were found. An analysis of the IFC data indicated that the gain of the two-parameter system and the counting rate were stable to less than 3%. Therefore, the data were scaled by an appropriate constant (1.42) to the count rate that was measured at the intermediate altitude of the Pfotzer maximum (~100 g/cm^2) to establish a base for comparison. The relative count rates obtained for the Compton electrons, recoil protons, and the neutron-produced secondary α particles were 142/10/1. The importance of these relative count rates and spectral shapes will be discussed later.

The pulse-height spectra of protons, α's, and Compton electrons are shown in Figs. 6(a), 6(b), and 6(c). Then the pulse-height spectrum for protons [Fig. 6(a)] was converted to the recoil-proton energy spectrum shown in Fig. 7. This conversation involves correcting for the nonlinearity of the flight pulse-height analyzer, for the dependence of scintillation light yield upon energy,[21] and for second scattering and wall effects.[22] For example, the channel width of the logarithmic PHA was 0.05 MeV at channel number 10 (3.6 MeV) and 0.50 MeV at channel number 60 (15.0 MeV). Consequently, the number of proton recoils per MeV was much larger

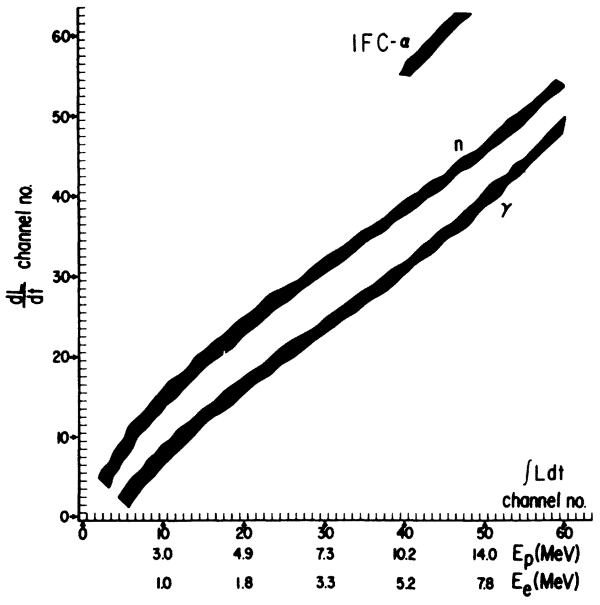

FIG. 3. A two-parameter (64 × 64) contour display of Compton electrons, recoil protons, and inflight calibrator (IFC) for a laboratory prototype. The widths of the dark bands are equal to one full width at half maximum (FWHM).

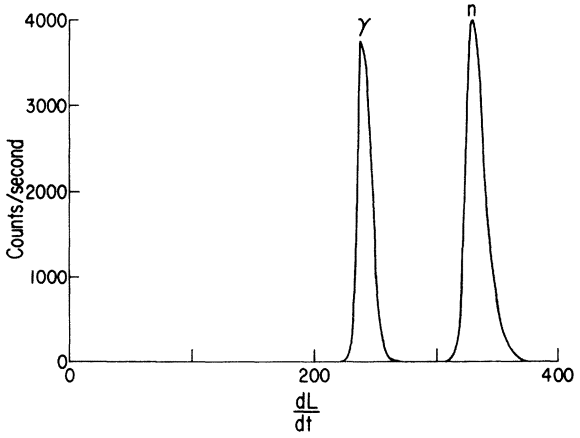

FIG. 4. A section of Fig. 3 taken at the $\int L\,dt$ value corresponding to the Compton edge of ^{60}Co.

in the lower flight channels.

The method of Broek and Anderson[22] was used to obtain the Pfotzer maximum neutron energy spectrum shown in Fig. 8. In this method the derivative $d/dE(dN_p/dE)$ as a function of E_p was evaluated from Fig. 7. The neutron energy spectrum (dN/dE) as a function of energy (E) was calculated from

$$dN/dE = -\frac{E}{n_H \sigma_{H(E)} L} F(E)^{-1} f(a(E)L)^{-1} \times d/dE(dN_p/dE), \quad (1)$$

where $a(E) = [n_C\sigma_C(E) + n_H\sigma_H(E)]$ is the total effective cross section in the scintillator, $\sigma_C(E)$ and $\sigma_H(E)$ are the total neutron scattering cross sections for carbon and hydrogen, respectively, L = the length of the scintillator, $F(E)$ = correction factor for the second-scattering and wall effects, and $f(a, L)$ = correction factor for the neutron flux attenuation in the scintillator. Typically $F(E) = 1.10$ at $E = 1.0$ MeV and $F(E) = 0.95$ at $E = 20$ MeV.[16] The correction factor $f(a(E), L)$ was closer to unity.[23]

Since approximately one-half the nuclei in the scintillator were carbon, an analysis of the effects of the carbon nuclei was necessary. There are two types of reactions with carbon that are important, $^{12}C(n, p)$ and $^{12}C(n, \alpha)$. The first reaction will produce a proton which complicates the unfolding procedure because the Borek-Anderson method was based upon protons from $H(n, p)$ reactions only. The relative proton contamination can be estimated from the $^{12}C(n, p)$ cross sections given by Kurz[24] and the atmospheric neutron energy spectrum of Lingenfelter[25]; it is less than 3% of the protons from the $H(n, p)$ reaction for protons of equal energy.

The possible contamination owing to the second reaction, $^{12}C(n, \alpha)$, was similarly estimated. There are two reaction channels through which these α's are produced: $C^{12}(n, \alpha)^9Be$ and $^{12}C(n, 3\alpha)n$. For the low-energy atmospheric neutrons $E_n \leq 14$ MeV, the first reaction predominates and above that energy the second reaction dominates. The α contamination from $^{12}C(n, \alpha)^9Be$ was found to be about 7% of the protons from $H(n, p)$ for particles which yield equal integrated ($\int L\,dt$) scintillations. In the flight data we were able to extract separately the secondary α particles from the recoil protons. We found that the relative α particle contribution was approximately 10%, which was in good agreement with the estimated contribution. It should be noted that since the α particles were pulse-shape-discriminated from protons in this experiment, these α's will not be counted as "protons."

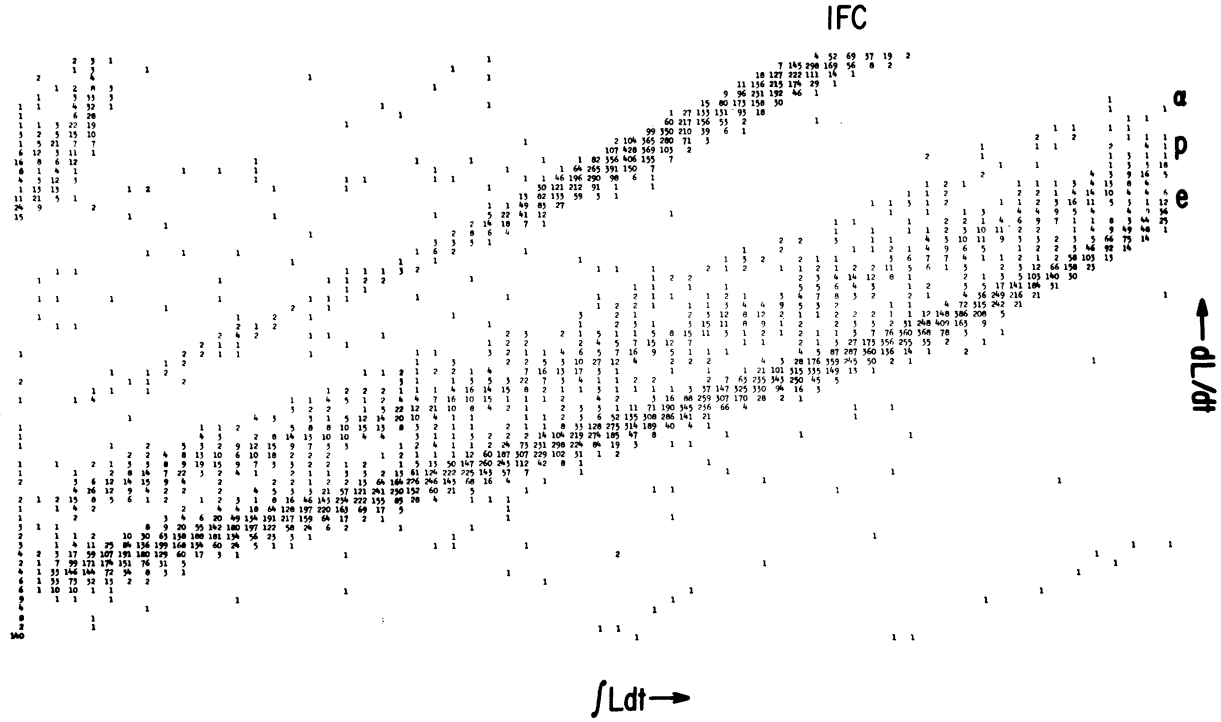

FIG. 5. Two-parameter ($\int L\,dt$ vs dL/dt) flight data taken from 541 to 62 mbar.

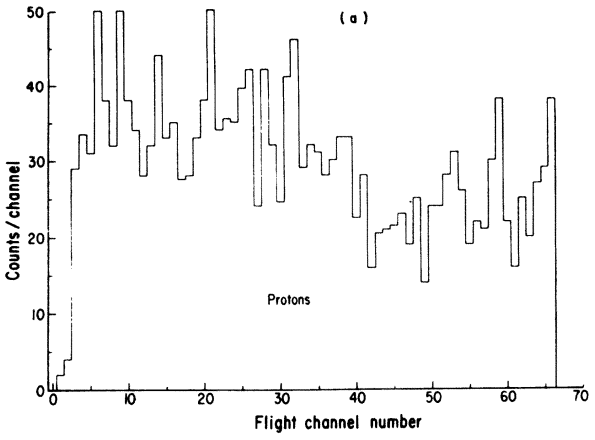

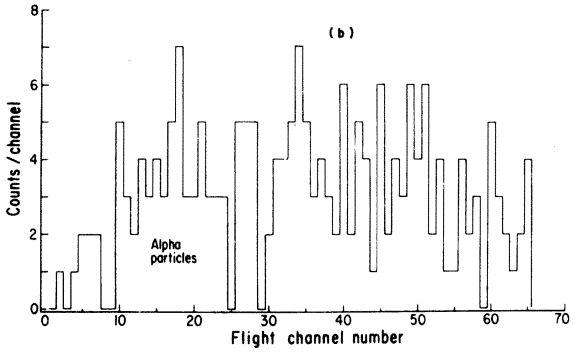

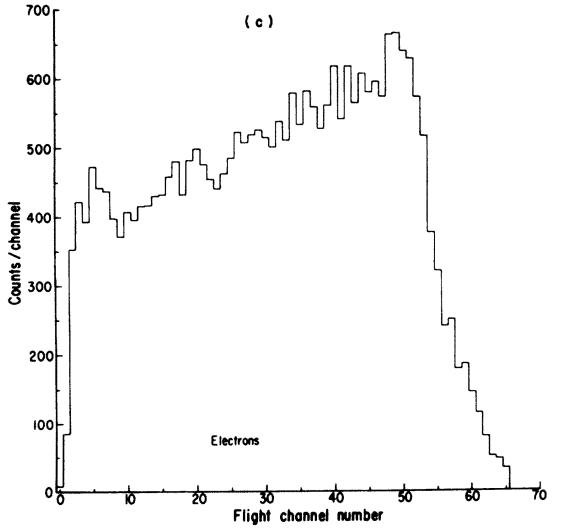

FIG. 6. (a) Recoil-proton count-rate data from Fig. 5. (b) The secondary alpha-particle spectrum extracted from Fig. 5. (c) The uncorrected Compton-electron spectrum taken from Fig. 5.

A high-precision neutron time-of-flight accelerator experiment recently completed in collaboration at the Michigan State University Cyclotron has similarly stressed the importance of a high-resolution two-parameter PSD. Four types of neutron-caused PSD effects have been resolved: $H(n, p)$, proton escapes from the scintillator, $^{12}C(n, p)$, and $^{12}C(n, \alpha)$.[26]

The unfolded differential neutron energy spectrum at Pfotzer maximum shown in Fig. 8 was fitted to a spectral shape of the form

$$dN/dE = BE^{-\beta}, \tag{2}$$

where β, the spectral parameter, is defined:

$$\beta = \frac{(d/-dE)(\ln dN/dE)}{(d/dE)(\ln E)}.$$

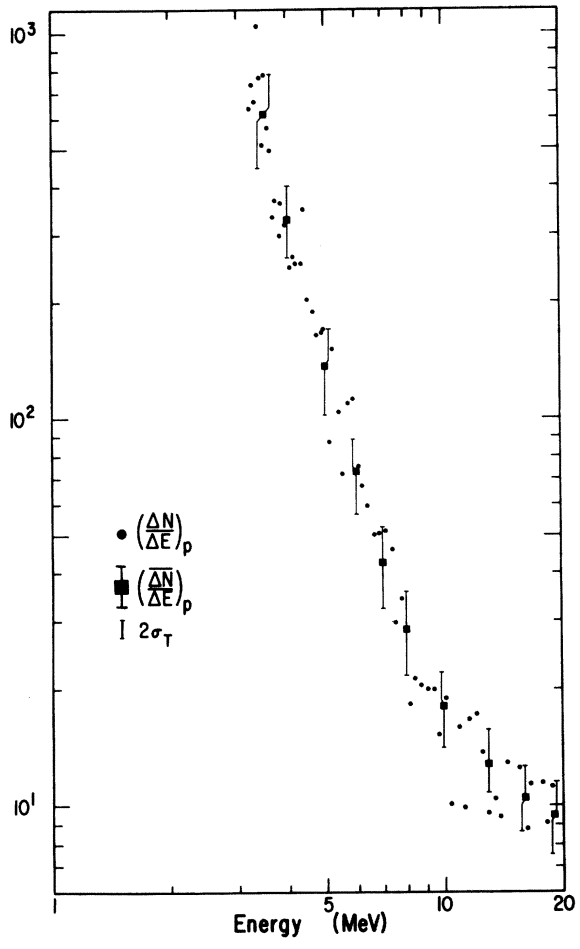

FIG. 7. The recoil-proton energy spectrum obtained from the data in Fig. 6(a). The larger dots are average values obtained by smoothing the data. To obtain the actual number of protons/MeV multiply the ordinate by 1.42.

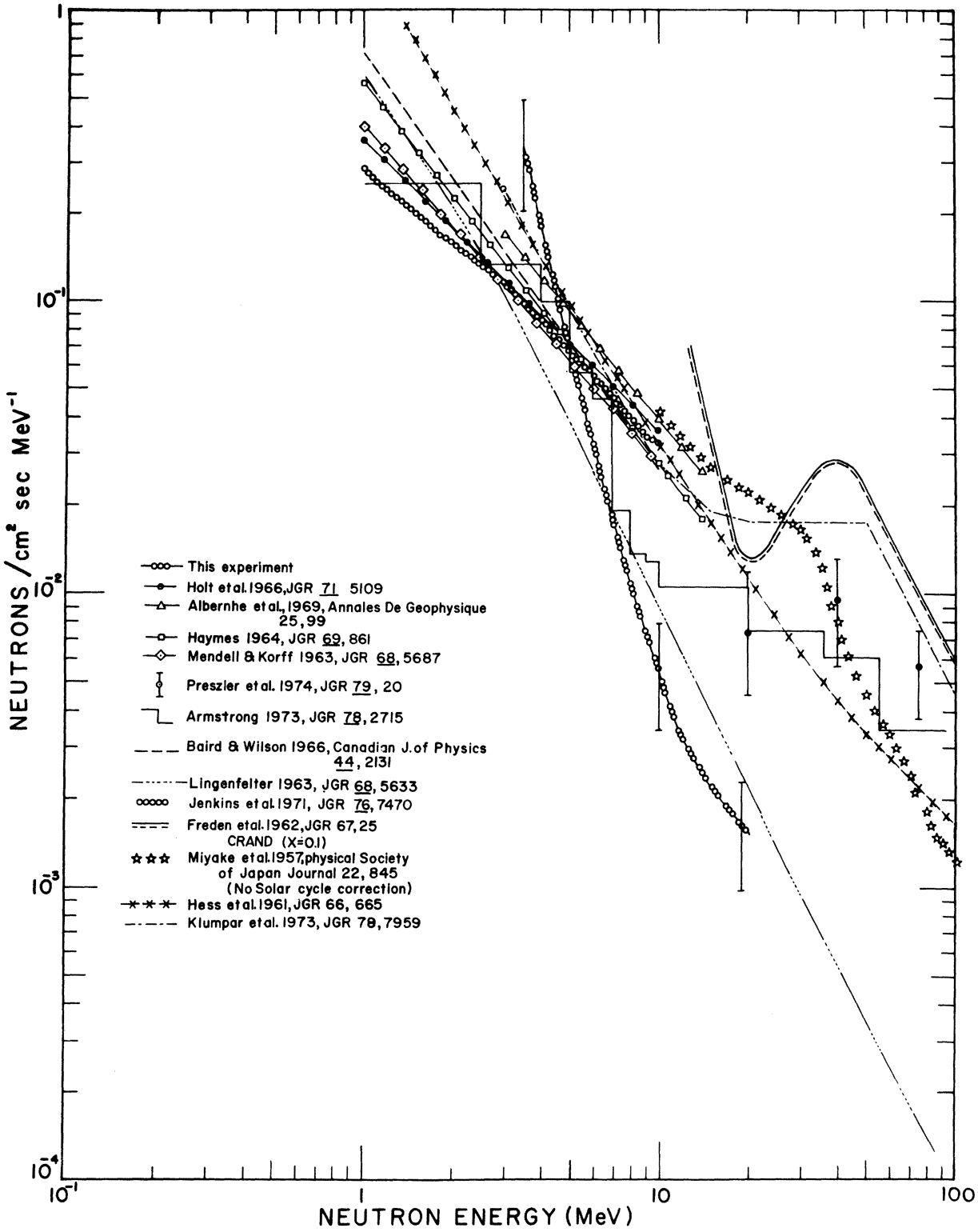

FIG. 8. The differential neutron energy spectrum at Pfotzer maximum. The error bars shown include statistical and systematic uncertainties as well as the uncertainty in determining the slope of the recoil-proton spectrum.

From a simple regression analysis on the 18 values of dN/dE deduced between 3.5 and 20 MeV, β was found to be 2.70 ± 0.16 as listed in Table I. The mean standard deviation $\bar{\sigma}$ of the observed from the calculated values for $\beta = 2.70$ was 26%, which is comparable to $\bar{\sigma} = 34\%$ based upon the estimated total experimental errors. Since it appears from Fig. 8 that β decreases smoothly with neutron energy E, the data were divided into three energy intervals: 3.5–6, 6–11, and 11–20 MeV. Then β was separately determined for each interval and the values are listed in Table I(b). Using the criterion based upon Gauss's mean square deviation, the $\bar{\sigma}$ for the three sections was 10%, indicating that β changes significantly with energy.

IV. DISCUSSION OF RESULTS

Since both the experimental technique used and the neutron energy spectrum are quite different from previous atmospheric neutron spectral measurements,[12-18,27-31] we believe that a consideration of the various possible difficulties in atmospheric neutron measurements is imperative. First, let us evaluate semiquantitatively the uncertainties in this experiment and, second, consider the possible difficulties encountered in fast-neutron measurements made in a background of charged particles and γ rays.

In this experiment the largest uncertainties in the proton-recoil spectrum shown in Fig. 7 arise from statistical and systematic errors. The statistical errors per channel are easily evaluated to be (15–20)%. The systematic errors, on the other hand, are much more difficult to evaluate. The main contribution comes from the differential nonlinearity of the logarithmic PHA in the lower channels. This is estimated to be comparable to the statistical errors for the lower channels of the flight PHA and considerably less than the statistical errors for the upper channels. The cross-calibration curve to convert the logarithmic PHA to a standard linear PHA that can then be converted easily to light units is shown in Fig. 9. Since the channel width is small in the lower channels, two criteria were used to minimize systematic errors. First, the derivative of the calibration curve must be smooth and nearly logarithmic. Second, the sum of all flight-channel widths must equal the total width of the single-channel analyzer constraining the $\int L\,dt$ range of the PHA. The error bars shown in Fig. 7 are the most probable values from combining these two major sources of error. To obtain the error bars shown in Fig. 8 the uncertainty in the slope of the proton-recoil spectrum was determined at the energies for which error bars are plotted.

Second, the most serious possible experimental difficulties in atmospheric neutron measurements can be attributed to one or more of the following: Compton electrons not being properly identified by the PSD, charged particles "leaking" through the anticoincidence system and thereby being falsely measured as neutrals, and the PSD falsely identifying neutron-produced secondary α particles as recoil protons. Each of these effects will both increase and harden the "measured" neutron energy spectrum. This can be seen by comparing Figs. 6(a), 6(b), and 6(c).

The effects of Compton electrons being mistakingly identified as protons by the PSD can be seen by comparing the relative intensities of Compton electrons and recoil protons as well as the shapes of the electron and proton pulse-height spectra. The Compton-electron pulse-height data of Fig. 6(c) are obviously a harder spectrum than the recoil-proton data of Fig. 6(a). Since the ratio of electrons to protons was 14.2, a 1% error in the PSD separation can produce a 14% error in the

TABLE I. Spectral parameter β as a function of neutron energy E.

Energy interval (MeV)	β
(a) 3.5–20	2.70 ± 0.16
(b) 3.5–6.0	4.4 ± 0.8
6–11	3.6 ± 0.6
11–20	1.5 ± 1.0

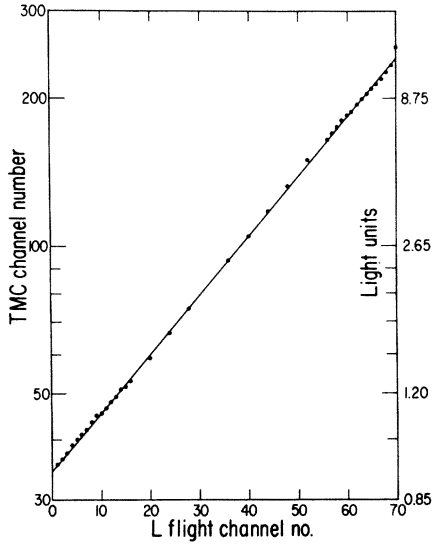

FIG. 9. The linear (Technical Measurement Corp.) channel number as a function of flight channel number of for $\int L\,dt$ pulses.

proton flux. The large difference in spectral shape can introduce a greater than 10% error in the slope β of the neutron energy spectrum for a 1% error in the PSD separation.

The second experimental uncertainty can be evaluated from the charged-particle pulse-height spectrum measured by the neutron detector when the flight charged-particle anticoincidence system was turned off. We observed that it was very similar in shape to the Compton-electron spectrum, i.e., a much harder and more intense spectrum than the recoil-proton spectrum. Therefore, the "leakage" of charged particles into the neutron detector will distort the same of the recoil-proton spectrum.

Third, if the PSD cannot separate α particles from recoil protons, both types of events are recorded as recoil protons. This would produce an increase of about 10% in the recoil-proton flux, as can be seen by comparing Figs. 6(a) and 6(b). This again yields a more intense neutron spectrum.

Another factor to be considered is the local production of neutrons and γ rays be cosmic rays interacting in the mass of the flight system. We used the technique of Boella *et al.*[27] and estimated local neutron production from the mass of the flight system outside of the anticoincidence shield to be 3.5×10^{-3} neutrons sec/cm^2, which is less than 0.1% of the ambient atmospheric neutron flux.[17] Another important contamination arises from the particles which were produced inside the charged-particle shield. Only protons need to be considered because the electrons so produced will be pulse-shape-discriminated. The proton contribution was estimated to be less than 2% assuming the most intense external atmospheric high-energy neutron spectrum measured by Preszler *et al.*[18]

V. CONCLUSIONS

We have found that the differential neutron energy spectrum at Pfotzer maximum at 42°N geomagnetic latitude was considerably steeper in the energy interval 3.5–10 MeV (Fig. 8) than previously measured spectra. The spectral parameter β for the differential neutron energy spectrum decreased from 4.4 ± 0.8 between 3.5 and 6.0 MeV to 1.5 ± 1.0 in the interval 11–20 MeV. The calculated neutron flux in the energy range 3.5 to 10 MeV was 0.36 ± 0.10 neutrons/cm^{2}sec, agreeing with that obtained earlier by Holt *et al.*[13] It is clear that the question of a possible change in the neutron energy spectrum between Pfotzer maximum and the top of the atmosphere remains unresolved. The intensity and shape of the neutron energy spectrum between 3–100 MeV is important to the evaluation of the contribution made by neutron leakage to the population of energic protons in the inner radiation belt. The results of the experiment show the necessity of using caution in interpreting earlier experiments and indicate that excellent PSD techniques must be used in atmospheric neutron measurements. Any linear extrapolations of the differential neutron energy spectrum to higher energies[8] cannot be justified.

ACKNOWLEDGMENTS

The assistance of L. Friling, D. Schow, and D. Huntley with the electronics design and construction is greatly appreciated. A. Buck and K. Pratt handled the data reduction. We are grateful to Dr. W. Burrus and Dr. V. V. Verbinski of Oak Ridge National Laboratory for many helpful discussions. This research was in partial fulfillment of the requirements of a Ph.D. degree and was supported by NASA under Contract No. NASr-164 and the Air Force under Contracts Nos. AF19(628)-2352 and F19628-68-C-0107. The research program was under the able direction of Dr. John A. Lockwood, whose many valuable suggestions are most sincerely acknowledged.

---

*Deceased, 1976. The final draft was edited by Dr. C. Y. Chen and Dr. J. A. Lockwood, University of New Hampshire.

[1]S. F. Singer, Phys. Rev. Lett. 1, 181 (1958).
[2]E. Schopper, E. Lohrmann, and G. Mauchk, *Encyclopedia of Physics* (Springer, New York, 1967), p. 372.
[3]J. A. Lockwood, Space Sci. Rev. 14, 663 (1973).
[4]W. N. Hess, Phys. Rev. Lett. 3, 1 (1959).
[5]L. I. Newkirk, J. Geophys. Res. 68, 1825 (1963).
[6]R. E. Lingenfelter, J. Geophys. Res. 68, 5633 (1963).
[7]A. J. Dragt, M. M. Austin, and R. S. White, J. Geophys. Res. 71, 1293 (1966).
[8]W. N. Hess and J. Killeen, J. Geophys. Res. 71, 2799 (1966).
[9]R. S. White, Rev. Geophys. Space Phys. 11, 595 (1973).
[10]J. A. Lockwood, C. Chen, L. Friling, and R. N. St. Onge, J. Geophys. Res. (to be published).
[11]G. Kanbach, C. Reppin, and V. Schonfelder, J. Geophys. Res. 79, 5159 (1974).
[12]R. C. Haymes, J. Geophys. Res. 69, 841 (1964).
[13]S. S. Holt, R. B. Mendell, and S. A. Korff, J. Geophys. Res. 71, 5109 (1966).
[14]R. B. Mendell and S. A. Korff, J. Geophys. Res. 68, 5487 (1963).
[15]F. Albernhe and R. Talon, Ann. Phys. (N.Y.) 28, 99 (1969).
[16]R. W. Jenkins, S. O. Ifedeli, J. A. Lockwood, and H. Razdan, J. Geophys. Res. 76, 7470 (1971).

[17]D. Klumpar, J. A. Lockwood, R. N. St. Onge, and L. A. Friling, J. Geophys. Res. 78, 7959 (1973).
[18]N. M. Preszler, G. M. Simmett, and R. S. White, J. Geophys. Res. 79, 20 (1974).
[19]R. N. St. Onge and J. A. Lockwood, Nucl. Instrum. Meth. 69, 347 (1969).
[20]R. N. St. Onge and J. A. Lockwood, Nucl. Instrum. Meth. 69, 25 (1969).
[21]V. V. Verbinski, W. R. Burrus, T. A. Love, W. Zobel, N. W. Hill, and R. Texter, Nucl. Instrum. Meth. 65, 8 (1968).
[22]H. W. Broek and C. E. Anderson, Rev. Sci. Inst. 31, 1063 (1960).
[23]J. B. Marion and J. L. Fowler, *Fast Neutron Physics* (Interscience, New York, 1960), Chap. 2B, p. 211.
[24]R. J. Kurz, Ph.D. thesis, University of California, Berkeley, 1964 (unpublished).
[25]R. E. Lingenfelter, Rev. Geophys. 1, 35 (1963).
[26]R. N. St. Onge, A. Galonsky, R. K. Jolly, and T. M. Amos, Nucl. Instrum. Meth. 126, 391 (1975).
[27]G. G. Boella, A. Degli, C. Dilworth, M. Panetti, and L. Scarsi, J. Geophys. Res. 70, 1019 (1965).
[28]T. W. Armstrong, K. C. Chandler, and J. Barish, J. Geophys. Res. 78, 2715 (1973).
[29]G. A. Baird and B. G. Wilson, Can. J. Phys. 44, 3131 (1966).
[30]S. C. Freden and R. S. White, J. Geophys. Res. 67, 25 (1962).
[31]S. Miyake and K. Hinotani, J. Phys. Soc. Japan 22, 845 (1957).
[32]W. N. Hess, J. Geophys. Res. 66, 665 (1961).